

RSC Advances



This is an *Accepted Manuscript*, which has been through the Royal Society of Chemistry peer review process and has been accepted for publication.

Accepted Manuscripts are published online shortly after acceptance, before technical editing, formatting and proof reading. Using this free service, authors can make their results available to the community, in citable form, before we publish the edited article. This *Accepted Manuscript* will be replaced by the edited, formatted and paginated article as soon as this is available.

You can find more information about *Accepted Manuscripts* in the [Information for Authors](#).

Please note that technical editing may introduce minor changes to the text and/or graphics, which may alter content. The journal's standard [Terms & Conditions](#) and the [Ethical guidelines](#) still apply. In no event shall the Royal Society of Chemistry be held responsible for any errors or omissions in this *Accepted Manuscript* or any consequences arising from the use of any information it contains.



Journal Name

ARTICLE

Novel β -FeOOH/NiO composite material as a potential catalyst for catalytic ozonation degradation of 4-chlorophenol

Ogheneochuko Oputu^a, Mahabubur Chowdhury^{b*}, Kudzanai Nyamayaro^a, Franscious Cummings^c, Veruscha Fester^a, Olalekan Fatoki^b

Received 00th January 20xx,
Accepted 00th January 20xx

DOI: 10.1039/x0xx00000x

www.rsc.org/

In this study we report on the organic linker mediated fabrication and catalytic activity of novel β -FeOOH/NiO composite material for the first time. Four-Chlorophenol (4-CP) was used as target molecule to evaluate the catalytic activity of the composite material in ozonation reactions. Three different β -FeOOH loadings, labelled 2, 5 and 10% β -FeOOH/NiO composite was prepared. 5% β -FeOOH/NiO composite material showed the highest activity in the composite structure. XRD, FTIR and TEM were used to characterise the composite structure. Evidence of chemically bonded interface between β -FeOOH and NiO was apparent from the FTIR and TEM results. Adsorption of 4-CP on the catalyst surface was found to be negligible. A first order reaction kinetics was used to describe the 4-CP degradation behaviour and the rate constants increased with increasing initial pH of the solution. No detectable amount of both Fe and Ni leaching into solution was observed at pH range of 10 – 2.3. After 20 min of ozonation reaction, 85% of 4-CP was removed by the heterogeneous system as opposed to 47% by ozonation alone. The developed composite material exhibited good recyclability as the catalytic activity of the material could be recovered by calcination after use. Maximum 66% of COD was removed just after 50 min of catalytic ozonation reaction. Enhanced catalytic activity of the composite material was due to higher generation of \cdot OH which was supported by photoluminescence (PL) experiments.

1. Introduction

The use of ozone as a chemical oxidant for organics in water has gathered wide spread research interest due to its stronger oxidizing power when compared to the more common chlorination and its avoidance of chlorinated by-products such as the chloromethanes. The industrial application of ozone for large-scale water treatment still faces certain problems; ozone oxidation is selective, and requires being produced in-situ via an expensive process. Also, recent work has shown that ozonation in the presence of bromine produces brominated by-products¹. The conversion of ozone to the unselective $\text{OH}\cdot$ gives better results for oxidation of organics, as the oxidizing power of $\text{OH}\cdot$ is higher than that of ozone. Research projects have therefore been geared towards the efficient conversion of ozone to $\text{OH}\cdot$ for application in water purification processes. Methods for achieving this objective includes, UV based break down of ozone to $\text{OH}\cdot$, application of ozone under high pH conditions, combining ozone with hydrogen peroxide and application of ozone in the presence of transition metal ions such as Fe^{2+} and Mn^{2+} to produce $\text{OH}\cdot$. While the application of metal ions and peroxide introduces unrecoverable reagents

consumed in the reaction process, the use of UV for ozone breakdown incurs additional cost to the water purification process. The use of heterogeneous catalyst offers an advantage over aforementioned processes, in that the ozone breakdown to $\text{OH}\cdot$ is via surface reaction mechanisms and therefore the catalyst can be recovered and recycled. Various metal oxides and metal oxides on metal oxide-supports surfaces such as; TiO_2 , MnO_2 , Al_2O_3 , $\text{Cu-Al}_2\text{O}_3$, Cu-TiO_2 , Ru-CeO_2 , VO/TiO_2 , VO-silica gel , $\text{TiO}_2\text{-Al}_2\text{O}_3$, ZnAl_2O_4 and $\text{Fe}_2\text{O}_3/\text{Al}_2\text{O}_3$ have been used to break down ozone to generate $\text{OH}\cdot$ ²⁻⁵.

Iron is an earth abundant material and has been recommended as a catalyst amongst many others. Many reports have been published that used iron based catalyst in ozonation process to remove various organic compounds, i.e. phenol, aniline, carboxylic acids, chlorobenzene, chlorophenols, dyes or natural organic matter⁶⁻¹⁰. Very little attention has been given towards iron oxy hydroxide materials despite their low toxicity and cheap and simple synthesis procedure. Catalytic properties of FeOOH based materials such as α -FeOOH¹⁰ and γ -FeOOH¹¹ have been reported before in the presence of H_2O_2 ¹. Catalytic ozonation of Nitrobenzene has been reported using α -FeOOH and β -FeOOH. However, Fe dissolution, weak catalytic activity and catalyst stability is still a challenge for iron based catalyst.

In our previous work¹², we demonstrated the effectiveness of ultra-small β -FeOOH nanorods¹³ in breaking down ozone to $\text{OH}\cdot$ thereby accelerating the rate of organic removal from

^a Department of chemistry, Cape Peninsula University of Technology, R.S.A
^b Flow process research centre, Cape Peninsula University of Technology, R.S.A.
Email-chowdhurym@cput.ac.za (Mahabubur Chowdhury*)
^c Electron Microscope Unit, University of the Western Cape, R.S.A

aqueous solution. The hetero-homo catalytic mechanism described in our paper was based on the surface acidic character of the hetero-FeOOH and a homogeneous catalytic process initiated at low pH by reduced Fe^{2+} ions. Due to the latter mechanism, catalyst loss during ozonation process was inevitable. Recently, Dong and co-authors prepared magnetic NiFe_2O_4 material for catalytic ozonation purposes^{14, 15}. The authors showed that NiFe_2O_4 material was stable and possessed enhanced charge transferability. No leaching of both metals was reported. In this current work, we incorporated NiO on β -FeOOH by forming hetero-junction via chemically bonded interface to reduce the loss of FeOOH as Fe^{2+} . This novel composite/ heterojunction structure material was subsequently tested for its catalytic property in ozone based oxidations of 4-Chlorophenol in aqueous medium. Leaching of both Fe and Ni were monitored during the reaction process and no dissolution of Fe and Ni was found in the solution. Catalyst recyclability was evaluated by reusing the catalyst three times without any calcination. Catalysts were rejuvenated by calcination at 250°C. Composite material showed good stability over the recycling period studied. The stability of the catalyst is based on the fact that Fe or Ni leaching was undetectable in the solution over repeated use of the catalyst. The composite material may therefore be considered superior to β -FeOOH in ozonation reactions as it does not suffer reductive dissolution and subsequent catalyst loss.

2. Experimental

2.1 Chemicals and materials

Analytical grade $\text{FeCl}_3 \cdot 6\text{H}_2\text{O}$, NH_4OH , ethanol (> 99 %), NiO nanopowder (<50 nm), 4-Chlorophenol, potassium iodide, coumarin (COU), 7-hydroxy coumarin (7-HC), sodium thiosulphate and tert-butanol (*t*-butanol) were purchased from sigma Aldrich South Africa and used as it is without any purification. Oxygen (99.998%) cylinder was obtained from "Air-Liquide" South Africa.

2.2 Synthesis of β -FeOOH

β -FeOOH nanorods were synthesised using the previously reported methods^{13, 16, 17}. For a typical synthesis 200 mL of deionized water was mixed with 200 mL of absolute ethanol. The pH of the solution was raised to 10 by drop wise addition of NH_4OH . 5 g of $\text{FeCl}_3 \cdot 6\text{H}_2\text{O}$ was added to the solution and stirred till dissolved. The final pH of the solution was approximately 2. The solution was placed in a Teflon lined pressure vessel and heated to 100 °C at 2 °C per minute and kept at that temperature for 2h. The pressure vessel was allowed to cool naturally after completion of the reaction followed by decantation of the supernatant liquid, centrifugation, washing of the solid with ethanol severally to remove residual chloride ions and storage in a desiccator.

2.3 Synthesis of β -FeOOH/NiO heterojunction composite material

Chemically bonded interface between NiO particles, with an average diameter of 50 nm, and β -FeOOH were formed using an organic binder. The method of preparation for β -FeOOH/NiO composite structure was adopted from previous study^{16, 18}. Three different mol % loading of β -FeOOH (2, 5 and 10%) on NiO was prepared. For a typical synthesis of 5 mol % β -FeOOH and 95 mol % NiO, (labelled as 5 % β -FeOOH/NiO) certain amount of β -FeOOH was suspended in 30 mL of ethanol. 10 mL of 0.1M maleic acid solution was added to the mixture. In a separate beaker 1g of NiO was dispersed in 30 mL ethanol. The two mixtures were stirred for 4h separately. After 4h the NiO mixture was added to the β -FeOOH mixture and stirred for 16h. The mixture was centrifuged, washed several times and dried overnight in air at 60 °C. The dried powder was annealed at 250 °C for 4h in an oven under air to decompose the organic components. Finally the annealed samples were treated under 9W UV light for 4h to remove any residual organic on the surface of the catalyst.

2.4 Characterization

The crystal structures of the synthesised products were determined using XRD, a Phillips PW 3830/40 Generator with Cu-K α radiation was used. The surface morphology of the synthesised crystals was studied using a Tecnai TF20 thermionic TEM, equipped with a LaB6 filament and a Gatan GIF energy filter. Images were captured at 200 keV in bright field mode. Selected area electron diffraction (SAED) patterns were obtained using the smallest area aperture available. EDX measurements were carried using TEM attachment. Infrared spectra were collected with a Perkin Elmer 1000 series FTIR spectrometer in the range of 4000-200 cm^{-1} in a KBr matrix. Photoluminescence (PL) was measured using a PerkinElmer LS55 luminescence spectrometer.

2.5 Ozonation degradation of 4-chlorophenol with the catalyst

For a typical experiment 0.01g of β -FeOOH/NiO were dispersed in 100 mL, 2×10^{-3} M 4-CP (water was used as solvent) solution by sonication. Dispersed β -FeOOH/NiO in 4-CP was fed in home made 200 mL glass reactor with a porous bubbler (porosity = 2). The initial pH of the solution was found to be ~7. The mixture was allowed to achieve adsorption equilibrium by stirring in the reactor without passage of O_3 gas. Aliquots were drawn for analysis at different time intervals to quantify 4-CP removal via adsorption. Once adsorption equilibrium has been reached a mixture of O_2 / O_3 was sparged into the glass reactor at a flow rate of 10 mL min^{-1} using a mass flow meter. Ozone concentration was kept constant at 28.24 mg/L, determined using indigo method¹⁹. Samples were withdrawn from the reactor at regular interval for 4-chlorophenol (4-CP) determination. The drawn samples were filtered using a 0.20 μm Pall Acrodisc GHP membrane filter and centrifuged at 10,000 rpm for 5 minutes. Preliminary tests were conducted to evaluate for 4-CP removal by adsorption through membrane filter. The membrane filter did not aid in the adsorption of 4-CP. 4-CP concentration was determined by liquid chromatography-mass spectroscopy (Agilent, LC-MS 6230), in negative mode, using a symmetry C8 column. The

mobile phase was 1% formic acid in water and acetonitrile; starting composition for the gradient was 85:15, 0:100 in 15 minutes at a flow rate of 0.4 mL min⁻¹. All LC-MS analysis was conducted immediately after sampling. All experiments were conducted in a repeated manner. Usage of ozone quenching agents (Na₂S₂O₃) was avoided during experimental runs to determine intermediates. It was done to prevent interference with LCMS results. Previous pilot LC-MS runs had shown that the stability of some intermediates did not exceed 6 hours. Repeated experiments were conducted for accurate intermediate identification purposes in this study.

3. Results and Discussion

3.1 Structural evaluation of the catalyst

XRD, TEM and FTIR were used to evaluate the structural characteristics of the materials. Fig-1a presents the XRD diffraction patterns of the pristine β -FeOOH (JCPDS, No. 42-1315), NiO (JCPDS, No. 071-1179) and composite materials prepared. However, the composite material does not show any β -FeOOH peaks in the X-ray diffraction patterns. This is due to the low loading of the β -FeOOH and high dispersion of the NiO on the β -FeOOH surface. Interestingly, the FWHM of the (200) plane of NiO increases with increasing β -FeOOH loading (Figure 1b). It implies the with β -FeOOH loading NiO crystal size decreases. This proves the incorporation of β -FeOOH in NiO or vice versa in the composite material, despite the absence of β -FeOOH peak in the X-ray diffraction pattern. FTIR spectra of the individual pristine materials and the composite materials were recorded and presented in Figure 1c. The broad band appeared at about 3550 and 1650 cm⁻¹ are related to the stretching and bending vibrations of the water molecules absorbed by the sample or KBr in all cases. The band at 1384.19 and 428 in the commercially purchased pristine NiO is attributed to the bending vibration of ionic CO₃²⁻ and Ni-O stretching of the octahedral NiO₆ groups respectively²⁰. For the pure β -FeOOH the absorptions peak at 851 and 681 cm⁻¹ is attributed to the Fe-O vibrational modes¹⁶. In fact the ionic radius of Fe³⁺ is similar to that of Ni²⁺ and the substitution of Fe in the NiO matrix can be speculated to be a favourable process. No significant difference was found in FTIR spectra of the three different % β -FeOOH loaded composite materials. Formation of interface / heterojunction between NiO and β -FeOOH was further verified from the TEM images (Figure 2 a&b). Corresponding EDS spectra (Figure 2a) shows the presence of both Ni and Fe in the composite material. The measured d-spacing of 2.3 and 2.09 nm measured from the HRTEM image (Figure 2b) in the β -FeOOH/NiO composite material corresponds to the (013) and (200) plane of pristine β -FeOOH and NiO respectively. This illustrates that successful heterojunction was formed between β -FeOOH and NiO. Dark-field scanning TEM (STEM) micrograph of a single β -FeOOH/NiO composite material was collected (Figure 2 c & d) with a high angular annular dark field (HAADF) detector at an electron probe size of approximately 0.7 nm for elemental mapping purposes. Elemental mapping was conducted to further confirm the presence of both Ni and Fe in the

heterojunction/composite structure (Figure 2c - e). Elemental mapping also confirms the high dispersion of NiO on β -FeOOH materials in the composite structure.

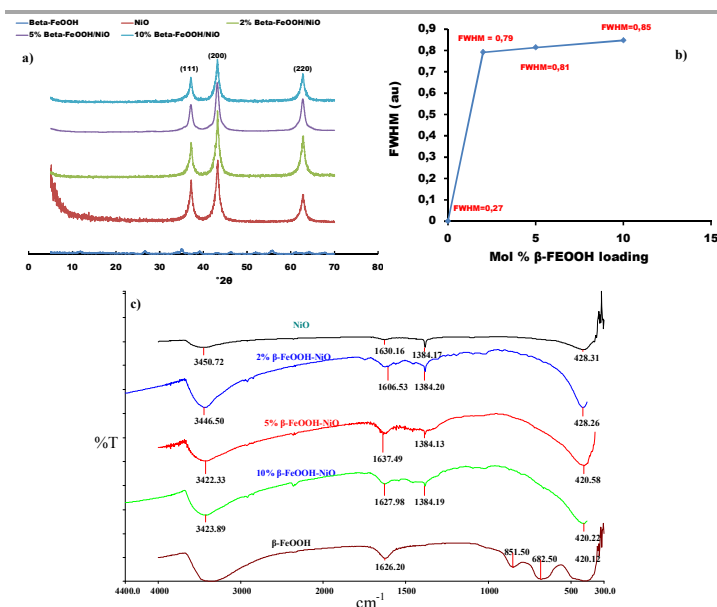


Figure 1: Catalyst characterization, a) XRD patterns of the materials, b) effect of β -FeOOH loading on the FWHM of the composite material and c) FTIR spectrum of the pristine β -FeOOH, NiO and the composite material

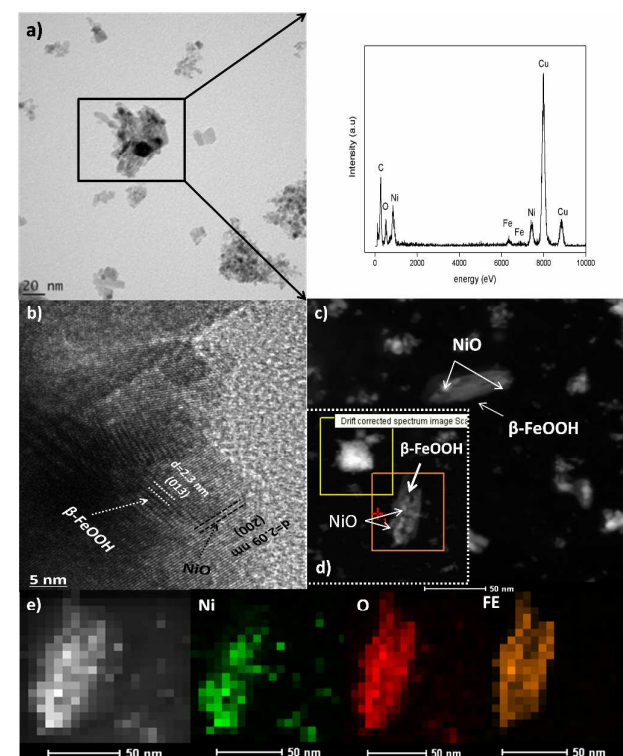


Figure 2: a) Bright-field TEM images of typical β -FeOOH/NiO composite material with corresponding EDS spectrum of the area of interest indicated by the box, b) HRTEM image of the composite material, c) Dark-field scanning TEM (STEM) micrograph of the composite material, d) area of interest in the yellow window was used to correct for

sample drift), e) The HAADF intensity of the area of interest as identified in (d) is shown in (e) with the corresponding elemental maps extracted.

3.2 catalytic activity of the β -FeOOH/ NiO composite material

Figure 3a and 3b presents the catalytic activity of the composite material, which was evaluated in terms of 4-CP removal. The catalytic effect of three different loading of β -FeOOH, i.e., 2, 5 and 10% in NiO labelled 2% β -FeOOH/NiO, 5% β -FeOOH/NiO and 10% β -FeOOH/NiO are presented in Figure 3a. It can be seen from Figure 3a that 5% β -FeOOH-NiO showed the highest catalytic activity compared to 2 and 10% β -FeOOH/NiO. It is well known that excessive or too little dopant can decrease the catalytic activity of the nanomaterial²¹. In our study, the 5% β -FeOOH loading in NiO was found to be optimum for enhanced catalytic activity in the presence of ozone. Hence, for all further studies only 5% β -FeOOH/NiO composite material was used. Pristine β -FeOOH in the presence of O_3 shows improved catalytic activity compared to NiO + O_3 system and O_3 alone. The composite material exhibits the highest catalytic activity (Figure 3b). After 20 min of reaction 85% of 4-CP was removed, when the composite material was used as a catalyst, compared to 66% of 4-CP when pristine β -FeOOH was used (Figure 3c). In the absence of ozone (in the presence of β -FeOOH/NiO only) negligible amount of 4-CP (3%) was removed, indicating that the role of adsorption on enhanced removal of 4-CP was minimal. Therefore the prepared β -FeOOH/NiO exhibits good catalytic behaviour for the ozonation degradation of 4-CP. 4-CP degradation kinetics were evaluated and presented in Figure 3d. First order reaction kinetics fitted well to describe the kinetic behaviour of 4-CP degradation via ozonation (O_3 only) and catalytic ozonation ($NiO+O_3$, β -FeOOH/NiO+ O_3). However, when β -FeOOH was used as a catalyst, the 4-CP degradation kinetics deviates from first order reaction kinetics due to dissolution of the catalyst as was shown earlier in our work¹². It is remarkable to note that addition of 5% β -FeOOH on NiO, the rate constant increased by more than 3 folds, from 0.066 to 0.212 for pristine NiO and 5% β -FeOOH/NiO respectively (Figure 3d insert). Atomic absorption spectroscopy (AAS) was used to measure the concentration of Fe and Ni in the solution during catalytic ozonation in the presence of the β -FeOOH/NiO composite material. No detectable amount of both Fe and Ni was found in the solution. Hence, it is suggested that NiO is a suitable and stable support for the β -FeOOH material which prevents the Fe^{2+} dissolution reaction which sets in at acidic pH. Reusability of a catalyst is very important from both a practical and economical point of view. The β -FeOOH/NiO composite material was recycled up to three times simply by filtering out the catalyst using a membrane filter and used in another batch of experiments without prior drying or calcination. Zhao and co-authors did a thorough study where they showed that low molecular carboxylic acids (generated as an intermediate during catalytic ozonation breakdown of phenolic compounds) has an affinity to the reactive centre of $NiFe_2O_4$ catalyst¹⁵. This leads to the accumulation of carboxylic acids on the catalyst surface and subsequent loss of catalytic efficiency. The catalytic degradation efficiency of as prepared

catalyst dropped to 54 % compared to 85% for the fresh catalyst after 20 minutes of reaction (Figure 4b) after the 3rd cycle. This may be due to the accumulation of low molecular weight carboxylic acids on catalyst surface as previously established in literature. In a separate study the catalyst were removed after the third cycle, dried overnight and calcined at 250°C to burn off accumulated carboxylic acids. The calcined catalyst showed degradation activity closed (79% 4-CP removal after 20 min of ozonation) to the fresh material (Figure 4a). Catalyst removal from the solution is still an issue, which limits the application of catalytic ozonation for environmental remediation purpose. We have evaluated the settling rate of the pristine β -FeOOH nanorods and β -FeOOH/NiO composite material in water in terms of turbidity. It can be seen from Figure 5a that the settling rate for β -FeOOH/NiO is significantly faster than pristine β -FeOOH. After 10h of sedimentation 96% of the composite material was settled compared to 2% of the pristine β -FeOOH nanorods that settled. Figure 5b presents a pictorial representation of the reactor setup after ozonation reaction for 50 min. The advantage of β -FeOOH composite material compared to pristine β -FeOOH material is clearly visible in Figure 5b. This implies that the catalyst can be recovered easily in a clarifier normally used in waste water treatment plant. This highlights the potential application of the composite material for industrial waste water treatment purposes. For comparative purposes, we incorporated β -FeOOH on Al_2O_3 and TiO_2 support. However, none of the other two supports (prepared via method described in the paper) showed appreciable catalytic activity for ozonation purposes.

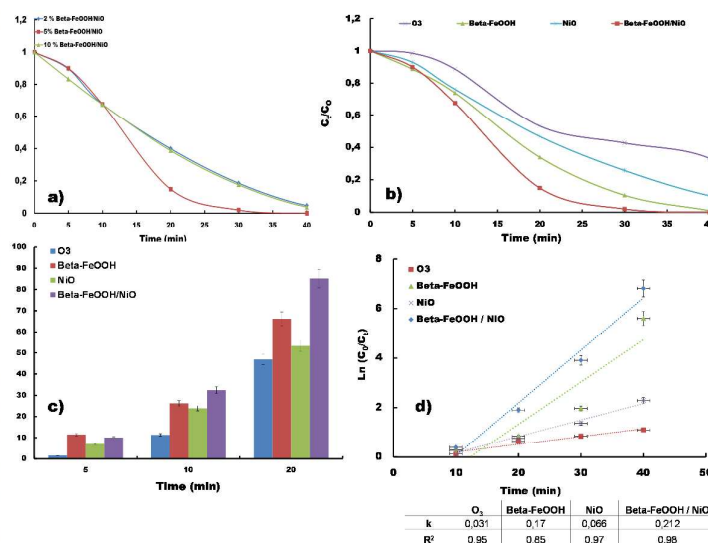


Figure 3: a) Effect of β -FeOOH loading on the catalytic activity of the β -FeOOH/NiO composite material, b) catalytic activity of the composite material compared to O_3 and pristine β -FeOOH and NiO, c) degradation efficiency of the composite material and d) 4-CP degradation kinetics [temperature = 20°C; initial pH = 7; initial 4-CP concentration = 2×10^{-3} M; catalyst load = 0.01g / 100 mL; O_3 dose = 0.6 mg.min⁻¹]

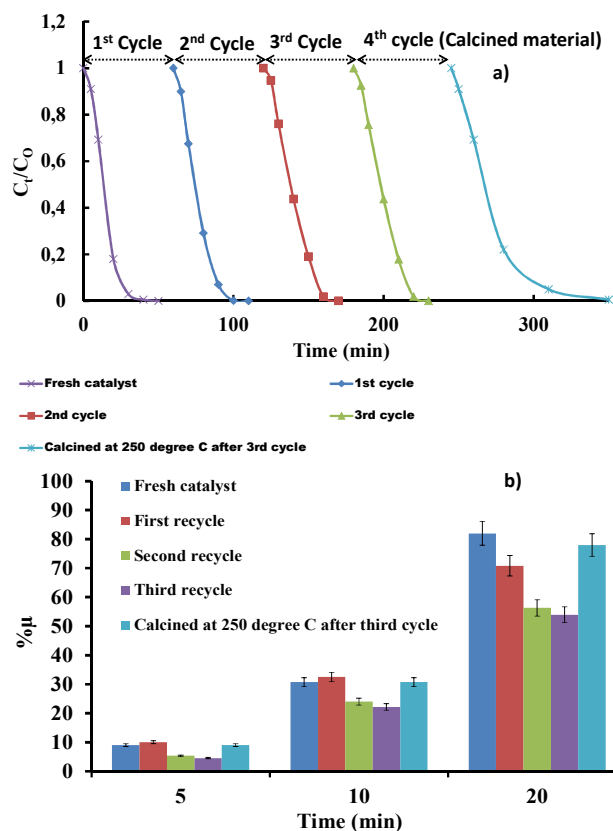
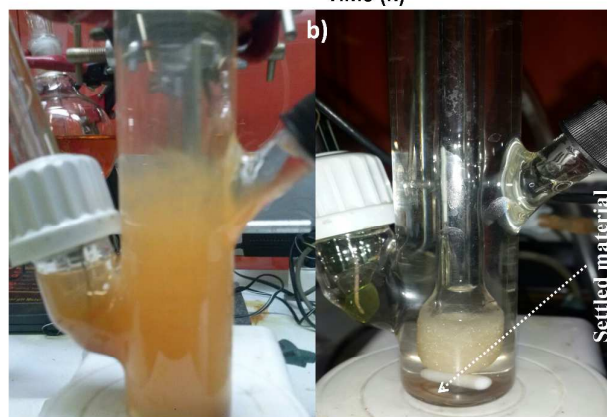
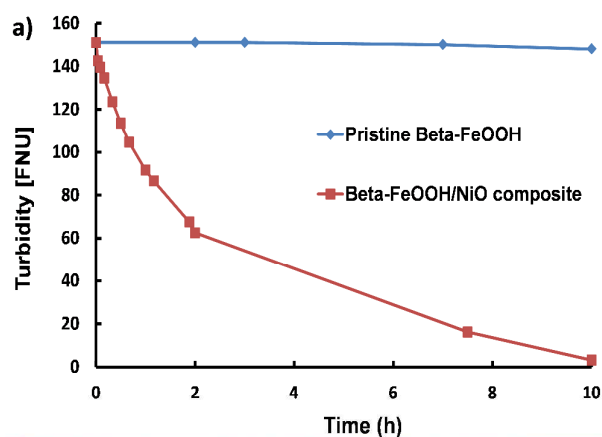


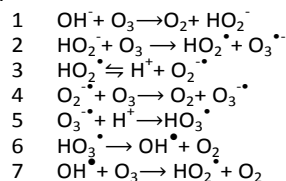
Figure 4: a) Performance of the catalyst after recycling & b) degradation efficiency after each recycling period [temperature = 20°C; initial pH = 7; initial 4-CP concentration = 2×10^{-3} M; catalyst load = 0.01 g / 100 mL; O_3 dose = 0.6 mg.min $^{-1}$]



0,01 g Pristine β -FeOOH after 10h post ozonation 0,01g β -FeOOH/NiO after 10h post ozonation

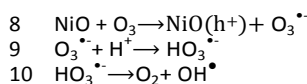
Figure 5: a) Sedimentation rate of pristine β -FeOOH and β -FeOOH/NiO composite material and b) reactor condition after 10h [50 min of ozonation reaction was carried and the material was allowed to settle]

In general degradation of organic compounds during catalytic ozonation occurs via adsorption, direct oxidative reaction by ozone and oxidative reaction by powerful non-selective hydroxyl radical, OH^\bullet . The total removal of organic compound is the sum of those by these three pathways. The composite material only adsorbed 3% of the 4-CP after 50 minutes in the absence of ozone. Hence, the role of adsorptive mechanism for the degradation of 4-CP was considered negligible. Enhanced degradation of 4-CP in the catalytic ozonation process is attributed to the presence of OH^\bullet . Generation of hydroxyl radical generally occurs due to interaction between ozone- OH^- (Equation 1-7) and ozone-metal oxides (Equation 8-14).



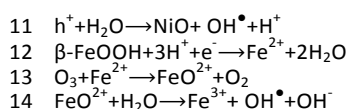
In the presence of the β -FeOOH/NiO composite material, OH^\bullet are produced in the bulk solution due to break down of ozone

on the catalyst surface. First, break down of ozone on the catalyst surface occur via the interaction of ozone with NiO due to its semiconductor properties²² and according to the reactions presented in Equation 8-10.



Equation 8-10 is supported by several studies²³⁻²⁵ and is plausible due to the electrophilic nature of $\text{O}_3^{\cdot-}$. However, in the presence of pristine NiO only 53% of 4-CP was degraded compared to 85% when the composite material was used as a catalyst. Various studies have reported that the presence of iron enhances the activity of ozone by increasing the concentration of OH^{\cdot} ²⁶⁻²⁸. The role of Fe can be related to firstly, the ability to accept valence band holes (in a heterojunction structure) and finally formation of FeO_2^+ species (From the interaction with O_3) which can produce OH^{\cdot} from water. The valence band edge potential of NiO and β -FeOOH are reported to be 3 and 2.5 eV, respectively^{16, 29}. Generated NiO valence band hole (Equation 8; due to the electrophilic nature of O_3) can be transferred to the valence band of the β -FeOOH material (via the heterojunction) due to difference in valence band edge potentials. The transferred holes can react with water to generate OH^{\cdot} (equation 11). Presence of too little Fe can hinder efficient hole transfer between NiO and β -FeOOH and excessive Fe can act as a hole trapping site^{30, 31}. This phenomenon can be speculated to be the reason for lower catalytic activity of 2% and 10% composite material. However, this subject requires further investigation.

Formation of OH^{\cdot} from β -FeOOH is also due to the following reaction (Equation 12-14):



Equation 12 is a common phenomenon for iron oxy-hydroxides type materials during oxidation of phenolic compounds and has been sustained in literature^{11, 32-35}, which normally leads to catalyst dissolution. The rate of reductive dissolution is dependent on the solution pH and organic reductant concentration³⁴. Note that the organic substrate serves as the source or required e^- in equation 12³⁴. The dissolution of pristine β -FeOOH as Fe^{2+} was shown in our previous study¹². Once Fe^{2+} is generated it either reacts with O_3 or detaches from the oxide surface which leaves a vacancy on the oxide surface i.e. surface dissolution. Fe^{2+} react with O_3 via equation 13 & 14 to generate OH^{\cdot} radicals. Generation of OH^{\cdot} via equation 8-14 was proved by photoluminescence (PL) technique, with coumarin (COU) as a fluorescence probe. COU reacts with OH^{\cdot} (Figure 6) to convert into highly luminescence 7-hydroxycoumarin (7-HC)³⁶. The concentration of 7-HC is proportional to the OH^{\cdot} concentration. An amount of 0.01g catalyst sample was dispersed in 100 mL of 1×10^{-3} M of COU

solution. Ozone was sparged through the reactor in the presence and absence of the catalyst. The sample was withdrawn at regular interval. It can be seen from Figure 7 that the rate of hydroxyl radical generation is higher in the presence of the composite catalyst compared to pristine β -FeOOH, NiO and ozone alone. However, the applied PL methods mainly detects free OH^{\cdot} in solution rather than surface bound OH^{\cdot} on catalyst surface³⁶. Hence, it can be implied that only a small fraction of OH^{\cdot} was detected and the formation rate of OH^{\cdot} is actually underestimated in the presence of a catalyst (Figure 7).

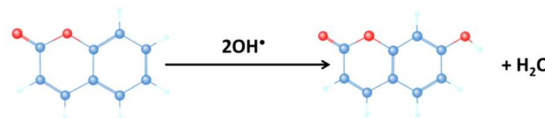


Figure 6: Conversion of COU to 7-HC in the presence of OH^{\cdot}

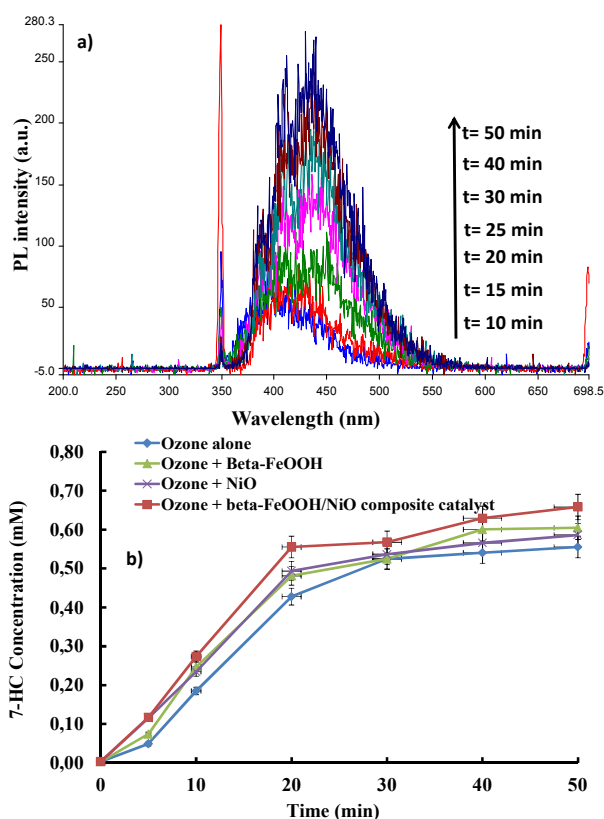


Figure 7: a) PL intensity changes observed during reaction in the presence of β -FeOOH/NiO composite catalyst and b) concentrations of 7-HC produced during the reaction

As previously mentioned no detectable amount of Fe-ions was found in the solution by AAS measurement (when β -FeOOH/NiO was used as a catalyst), this confirms that Fe dissolution did not take place. Therefore, it is suggested that reaction between Fe^{2+} and O_3 (Equation 13) is kinetically faster than that of Fe^{2+} dissolution reaction (Equation 12) in the composite material. Similar inter-conversion of Fe^{2+} to Fe^{3+} in

the presence of an oxidant (H_2O_2) and reductant (4-CP) has been previously identified and explained by Bandara and co-authors³⁷. The absence of Fe dissolution explains the composite materials good recycling ability as shown in Figure 4. In a control experiment a radical scavenger, tert-butanol (*t*-butanol; 2×10^{-2} M) were added to the 4-CP solution to evaluate the effect of oxidation via hydroxyl radical. The presence of *t*-butanol decreased the 4-CP removal efficiency significantly, and the degradation efficiency was only ~50% after 20 min (Figure 8). This value was much lower than that (85%) without *t*-butanol, proving the significant role of radicals OH^\bullet in the degradation of 4-CP.

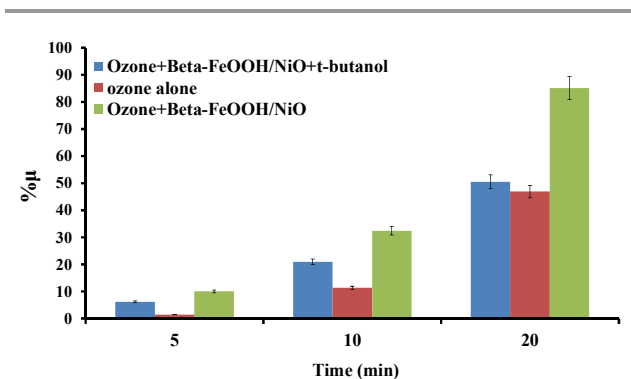


Figure 8: Role of OH^\bullet on the degradation of 4-CP [temperature = 20 °C; initial pH = 7; initial 4-CP concentration = 2×10^{-3} M; catalyst load = 0.01 g / 100 mL; O_3 dose = 0.6 $\text{mg} \cdot \text{min}^{-1}$, *t*-butanol concentration = 2×10^{-2} M]

The intermediate products obtained during ozonation of 4-CP using pristine $\beta\text{-FeOOH}$ and $\beta\text{-FeOOH}/\text{NiO}$ composite material was identical. A scheme depicting the oxidation process with and without catalyst as followed by LC-MS is presented in Figure 9. Several authors have reported on the oxidation (via ozone and other method) products of 4-CP²⁸. In an extensive work by Li and co-authors, oxidation of 4-CP was described by two path ways; i.e., the hydroquinone path way and 4-chlorocatechol pathway^{38, 39}. The authors also proved that the presence of heterogeneous catalyst promotes the 4-chlorocatechol path way. It can be seen from Figure 9 that when only ozone was used benzoquinone ($\text{C}_6\text{H}_4\text{O}_2$) was observed after 5 minutes of 4-CP oxidation. However, no $\text{C}_6\text{H}_4\text{O}_2$ was observed in the heterogeneous catalytic system. Hence, we postulated that the use of the ozone alone and ozone + catalyst promoted the oxidation of 4-CP via hydroquinone and 4-chlorocatechol (i.e. hydroxylation and dechlorination) pathway, respectively. Note that hydroquinone is unstable and is readily converted to benzoquinone. In the presence of O_3 alone, a compound $\text{C}_6\text{H}_5\text{ClO}_2$, was detected after 10 minutes. Saulea and Brillas argued that this compound was an isomer of 4-chlorocatechol obtained by hydroxylation of 4-CP at the meta position²⁸. Very important difference in the two mentioned oxidations route is the avoidance of the dimer ($\text{C}_{12}\text{H}_8\text{Cl}_2\text{O}_2$) and the trimeric oxidation product ($\text{C}_{18}\text{H}_3\text{O}_5$) in the catalytic oxidation route. It must be stated here that converse to previous report⁴⁰, both routes observed in our study do not proceed via dechlorination as the

first step. Both reaction path ways subsequently generates $\text{C}_5\text{H}_4\text{O}_2$ and other previously reported compounds, e.g. $\text{C}_6\text{H}_4\text{O}_4$. The mechanistic pathways involved in both process (homogeneous and heterogeneous) is the subject of our subsequent study, hence not fully discussed here. Mass spectrum data of identified compounds can be found in the supporting documents.

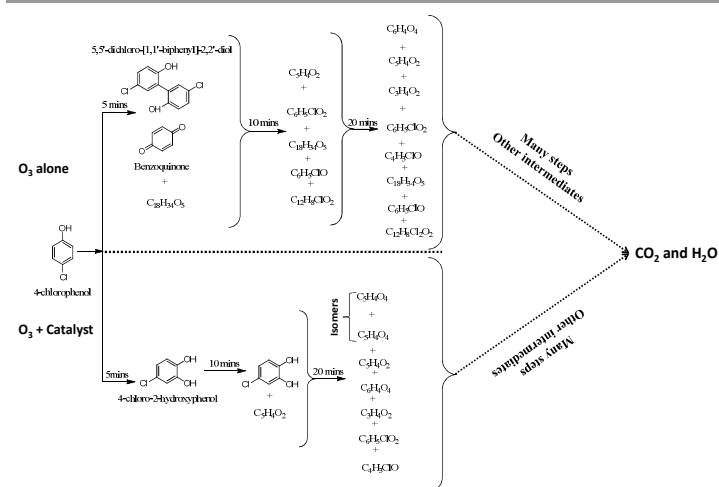


Figure 9: Proposed schematic representation of 4-CP oxidation pathway

3.3 Effect of processing parameters on 4-CP degradation

3.3.1 Effect of catalyst load

From an environmental point of view, conversion of any organic pollutant, as 4-CP, is only the first step in the ultimate objective, i.e., to attain the mineralization of the emerging solutions. On such a note, further experiments were conducted at increased dose of $\beta\text{-FeOOH}/\text{NiO}$ composite, 0.05 g and 0.1 g to evaluate the removal of chemical oxygen demand (COD). Increasing catalyst load brought about a decrease in 4-CP degradation (Fig 10a). This is attributed to the fact that the small sized particles agglomerated with increase in catalyst load and subsequently reduces reaction surface area between catalyst and O_3 . The rate constant for 4-CP degradation, k , decreased significantly from 0.21 to 0.13 min^{-1} when the catalyst load was increased from 0.01 to 0.05 g/L respectively. Further increase in catalyst load to 0.1 g/L did not affect the rate constant significantly ($k = 0.11 \text{ min}^{-1}$). However the rate constant also decreased when the catalyst concentration was 0.005 g/L (data not shown). Hence, catalyst load of 0.01 g/L was found to be optimum in this study. Similar trend was observed for COD removal also. Maximum and minimum of 66% and 51% of COD was removed for a catalyst load of 0.01 and 0.1g/L respectively after 50 min of reaction (Figure 10b). The cheap and simple synthesis technique, catalyst stability and ability to mineralize 4-CP within short period of time might make the $\beta\text{-FeOOH}$ supported NiO composite material a potential catalyst for ozonation purpose.

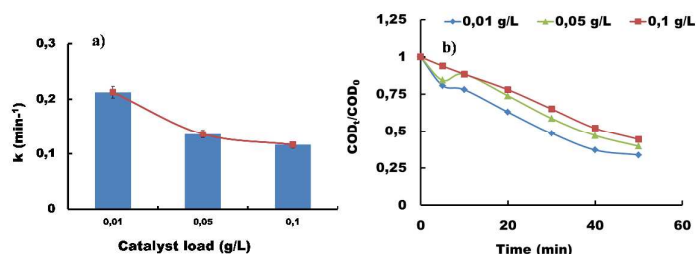


Figure 10: Dependence of a) rate constant and b) COD removal on catalyst load [temperature = 20°C; initial pH = 7; initial 4-Cp concentration = 2×10^{-3} M; O_3 dose = $0.6 \text{ mg} \cdot \text{min}^{-1}$]

3.3.2 Effect of initial pH on the 4-CP degradation

Figure 11a shows that with increasing initial solution pH, 4-CP degradation rate constant increases in the presence of β -FeOOH/NiO composite material. The solution pH is normally ~ 7 before the introduction of ozone. A decrease in initial solution pH to 3 decreased the 4-CP degradation rate constant significantly. However, increase of initial solution pH from 7 to 10 did not increase the rate constant greatly. It is well known that application of ozone under high pH conditions generally increases the OH^\bullet production. It can be seen from figure 11a that in all cases the degradation rate constant is higher in the presence of the β -FeOOH/NiO composite material, successfully highlighting the efficient catalytic activity. The initial pH values were observed to decrease (Figure 11b) during the 4-CP degradation and shift towards more acidic pH values as the reaction proceeds. This is due to the generation of low molecular weight carboxylic acids during the degradation process as stated in earlier section. Dissolution of Fe during ozonation at acidic condition is a common phenomenon and have been reported in many places in the literature^{6, 11, 37}. Figure 11c shows that the 4-CP degradation kinetics in the presence of β -FeOOH/NiO follows a 1st order reaction kinetics. When pristine β -FeOOH was used as a catalyst the reaction kinetics deviated from first order reaction kinetics and a two stage first order reaction kinetics was used to describe the reaction behaviour. Previously two-stage mechanism has been identified and was used to describe the kinetics of peroxide decomposition on lepidocrocite surface¹¹. The first stage (Figure 11d) has a lower rate constant ($k = 0.054 \text{ min}^{-1}$) because heterogeneous catalysis dominates here while the second stage has a higher rate constant ($k = 0.235 \text{ min}^{-1}$), as homogeneous catalysis is dominant because of β -FeOOH dissolution¹². However, in the presence of β -FeOOH/NiO composite catalyst this kind of behaviour was not observed. This suggests that by incorporating the β -FeOOH in NiO support the Fe dissolution was prevented and also the 4-CP degradation efficiency was enhanced.

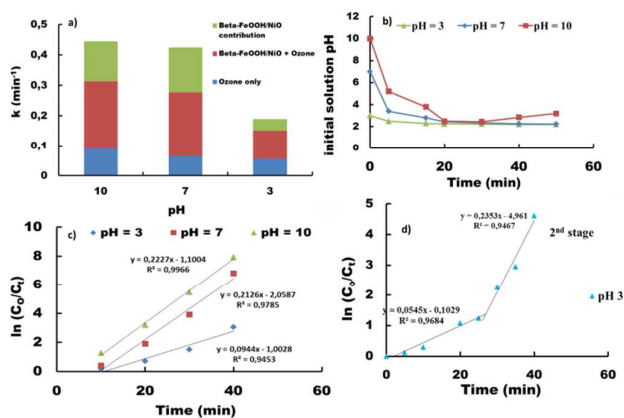


Figure 11: a) Dependence of rate constant on initial pH, b) decrease in solution pH with time, c) degradation kinetics of 4-CP at various pH in the presence of the composite materials and d) degradation kinetics of 4-CP at low pH in the presence of pristine β -FeOOH. [temperature = 20°C; initial 4-Cp concentration = 2×10^{-3} M; catalyst load = $0.01 \text{ g} / 100 \text{ mL}$; O_3 dose = $0.6 \text{ mg} \cdot \text{min}^{-1}$]

4. Conclusions

The ozonation of 4-CP, a recalcitrant organic compound is significantly improved in the presence of a novel β -FeOOH/NiO composite catalyst. Chemically bonded interface between β -FeOOH nanorods and NiO were created via organic linker mediated route. From the FTIR results and TEM images it was evident that the β -FeOOH nanorods successfully dispersed itself in the NiO matrix. Amount of β -FeOOH loading had an effect on the catalytic efficiency of β -FeOOH/NiO composite material. An optimum loading of 5% β -FeOOH in NiO showed the highest catalytic activity during the catalytic ozonation of 4-CP. Adsorption of 4-CP on the catalyst surface was found to be negligible. After 20 minute of reaction 85% of 4-CP was removed. The catalyst was recycled up to three times and was rejuvenated upon calcining. Maximum of 66% COD was removed using $0.1 \text{ g} / 100 \text{ mL}$ catalyst load. Degradation of 4-CP primarily occurs on the catalyst surface. The degradation follows a first order reaction kinetics and the rate constants increased with increasing initial pH of the solution in this heterogeneous catalytic system. No detectable amount of both Fe and Ni leaching into solution was observed at acidic pH. This highlights the potential application of this catalyst in ozonation treatment of industrial waste water that contains organic compounds.

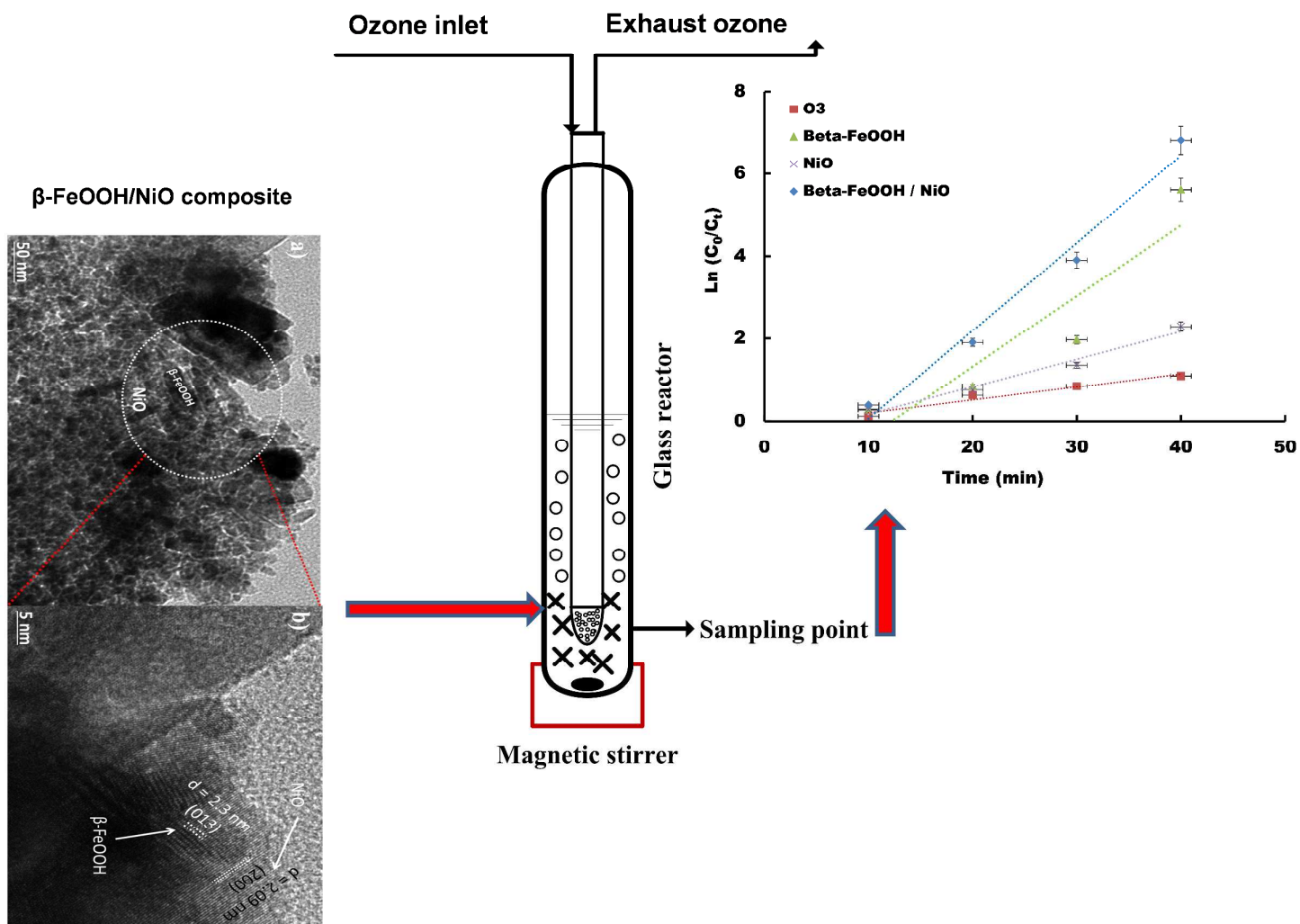
Acknowledgements

This work was supported by the National Research Foundation (Grant no: 88220) of South Africa and Cape Peninsula university of Technology.

Notes and references

1. Y. Nie, C. Hu, N. Li, L. Yang and J. Qu, *Applied Catalysis B: Environmental*, 2014, 147, 287-292.

- 2.B. Kasprzyk-Hordern, M. Ziólek and J. Nawrocki, *Applied Catalysis B: Environmental*, 2003, 46, 639-669.
- 3.Y. Dong, H. Yang, K. He, S. Song and A. Zhang, *Applied Catalysis B: Environmental*, 2009, 85, 155-161.
- 4.Y. Dong, K. Li, P. Jiang, G. Wang, H. Miao, J. Zhang and C. Zhang, *RSC Advances*, 2014, 4, 39167-39173.
- 5.H. Zhao, Y. Dong, P. Jiang, G. Wang, J. Zhang and C. Zhang, *Chemical Engineering Journal*, 2015, 260, 623-630.
- 6.F. J. Beltrán, F. J. Rivas and R. Montero-de-Espinosa, *Water Research*, 2005, 39, 3553-3564.
- 7.N. Al-Hayek, B. Legube and M. Doré, *Environmental Technology Letters*, 1989, 10, 415-426.
- 8.C. Cooper and R. Burch, *Water Research*, 1999, 33, 3695-3700.
- 9.M. M. Hassan and C. J. Hawkyard, *Catalysis Communications*, 2002, 3, 281-286.
- 10.J.-S. Park, H. Choi and J. Cho, *Water Research*, 2004, 38, 2285-2292.
- 11.S. Chou and C. Huang, *Chemosphere*, 1999, 38, 2719-2731.
- 12.O. Oputu, M. Chowdhury, K. Nyamayaro, O. Fatoki and V. Fester, *Journal of environmental sciences*, 2015.
- 13.M. Chowdhury, V. Fester, G. Kale and O. Cespedes, *Journal of Nanoparticle Research*, 2014, 16, 1-11.
- 14.H. Zhao, Y. Dong, G. Wang, P. Jiang, J. Zhang, L. Wu and K. Li, *Chemical Engineering Journal*, 2013, 219, 295-302.
- 15.H. Zhao, Y. Dong, P. Jiang, G. Wang, J. Zhang and K. Li, *Catalysis Science & Technology*, 2014, 4, 494-501.
- 16.M. Chowdhury, M. Ntiribinyange, K. Nyamayaro and V. Fester, *Materials Research Bulletin*, 2015, 68, 133-141.
- 17.M. Chowdhury, V. Fester and G. Kale, *Journal of Crystal Growth*, 2014, 387, 57-65.
- 18.S. B. Rawal, A. K. Chakraborty and W. I. Lee, *Bull. Korean Chem. Soc*, 2009, 30.
- 19.H. Bader and J. Hoigné, *Water Research*, 1981, 15, 449-456.
- 20.Y. Bahari Molla Mahaleh, S. K. Sadrnezhad and D. Hosseini, *Journal of Nanomaterials*, 2008, 2008, 4.
- 21.Q. Dai, J. Wang, J. Chen and J. Chen, *Separation and Purification Technology*, 2014, 127, 112-120.
- 22.S. M. Avramescu, C. Bradu, I. Udrea, N. Mihalache and F. Ruta, *Catalysis Communications*, 2008, 9, 2386-2391.
- 23.R. Gracia, S. Cortés, J. Sarasa, P. Ormad and J. L. Ovelleiro, *Ozone: Science & Engineering*, 2000, 22, 461-471.
- 24.B. Dhandapani and S. T. Oyama, *Applied Catalysis B: Environmental*, 1997, 11, 129-166.
- 25.S. Imamura, M. Ikebata, T. Ito and T. Ogita, *Industrial & Engineering Chemistry Research*, 1991, 30, 217-221.
- 26.J. Villaseñor, P. Reyes and G. Pecchi, *Catalysis Today*, 2002, 76, 121-131.
- 27.G. Ruppert, R. Bauer and G. Heisler, *Chemosphere*, 1994, 28, 1447-1454.
- 28.R. Sauleda and E. Brillas, *Applied Catalysis B: Environmental*, 2001, 29, 135-145.
- 29.Y. Xu and M. A. A. Schoonen, *American mineralogist*, 2000, 85, 543-556.
30. M. Nishikawa, Y. Mitani and Y. Nosaka, *The Journal of Physical Chemistry C*, 2012, 116, 14900-14907.
31. J. Zhu, F. Chen, J. Zhang, H. Chen and M. Anpo, *Journal of Photochemistry and Photobiology A: Chemistry*, 2006, 180, 196-204.
32. W. Stumm and B. Sulzberger, *Geochimica et Cosmochimica Acta*, 1992, 56, 3233-3257.
33. A. Vértes and I. Czakó-Nagy, *Electrochimica Acta*, 1989, 34, 721-758.
34. A. T. Stone, *Environmental Science & Technology*, 1987, 21, 979-988.
35. W. Stumm and J. Morgan, *Aquatic Chemistry*, Wiley-Interscience, New York, 2nd edn., 1981.
36. Q. Xiang, J. Yu and P. K. Wong, *Journal of Colloid and Interface Science*, 2011, 357, 163-167.
37. J. Bandara, U. Klehm and J. Kiwi, *Applied Catalysis B: Environmental*, 2007, 76, 73-81.
38. X. Li, J. W. Cubbage, T. A. Tetzlaff and W. S. Jenks, *The Journal of Organic Chemistry*, 1999, 64, 8509-8524.
39. X. Li, J. W. Cubbage and W. S. Jenks, *The Journal of Organic Chemistry*, 1999, 64, 8525-8536.
40. X.-w. Xu, X.-h. Xu, H.-x. Shi and d.-h. Wang, *Journal of Zhejiang University SCIENCE*, 2005, 6B, 553-558.



Graphical abstract